Short Article

Developmental Cell

The Role of Transcription Factors and Nuclear Pore Proteins in Controlling the Spatial Organization of the Yeast Genome

Highlights

- Interaction of Gcn4 target genes involves a direct role for Gcn4 and Nup2
- Gcn4's "positioning domain" promotes NPC interaction and stronger transcription
- Most yeast transcription factors promote targeting to the NPC
- Targeting occurs by two distinct pathways: Nup100 dependent and Nup100 independent

Authors

Donna Garvey Brickner, Carlo Randise-Hinchliff, Marine Lebrun Corbin, ..., Subin Hwang, Raven Watson, Jason H. Brickner

Correspondence

j-brickner@northwestern.edu

In Brief

Brickner et al. show that transcription factors (TFs) control positioning of genes through interaction with the nuclear pore complex. A "positioning domain" from one TF promotes interaction with the pore, and a global screen reveals that most yeast TFs mediate targeting to the NPC using at least two different pathways.

Brickner et al., 2019, Developmental Cell *49*, 936–947
June 17, 2019
https://doi.org/10.1016/j.devcel.2019.05.023

CellPress

CellPress

Developmental Cell
Short Article

The Role of Transcription Factors and Nuclear Pore Proteins in Controlling the Spatial Organization of the Yeast Genome

Donna Garvey Brickner,[1,2] Carlo Randise-Hinchliff,[1,2,3] Marine Lebrun Corbin,[1] Julie Ming Liang,[1] Stephanie Kim,[1] Bethany Sump,[1] Agustina D'Urso,[1,4] Seo Hyun Kim,[1] Atsushi Satomura,[1] Heidi Schmit,[1] Robert Coukos,[1,5] Subin Hwang,[1] Raven Watson,[1] and Jason H. Brickner[1,6,*]

[1]Department of Molecular Biosciences, Northwestern University, Evanston, IL 60201, USA
[2]These authors contributed equally
[3]Present address: Illumina, San Diego, CA, USA
[4]Present address: Division of Biological Sciences, University of California, San Diego, La Jolla, CA, USA
[5]Present address: Department of Genetics, Stanford University School of Medicine, Stanford, CA, USA
[6]Lead Contact
*Correspondence: j-brickner@northwestern.edu
https://doi.org/10.1016/j.devcel.2019.05.023

SUMMARY

Loss of nuclear pore complex (NPC) proteins, transcription factors (TFs), histone modification enzymes, Mediator, and factors involved in mRNA export disrupts the physical interaction of chromosomal sites with NPCs. Conditional inactivation and ectopic tethering experiments support a direct role for the TFs Gcn4 and Nup2 in mediating interaction with the NPC but suggest an indirect role for factors involved in mRNA export or transcription. A conserved "positioning domain" within Gcn4 controls interaction with the NPC and inter-chromosomal clustering and promotes transcription of target genes. Such a function may be quite common; a comprehensive screen reveals that tethering of most yeast TFs is sufficient to promote targeting to the NPC. While some TFs require Nup100, others do not, suggesting two distinct targeting mechanisms. These results highlight an important and underappreciated function of TFs in controlling the spatial organization of the yeast genome through interaction with the NPC.

INTRODUCTION

In eukaryotic cells, the spatial arrangement of chromosomes and genes within the nucleus is non-random (Bickmore and van Steensel, 2013; Parada et al., 2004). Interphase chromosomes are positioned non-randomly with respect to nuclear landmarks such as the nuclear envelope (Cremer and Cremer, 2010), in part because of the physical interaction of chromosomal loci with stable structures such as the nuclear lamina or nuclear pore complexes (NPCs; Brickner, 2017; Ibarra and Hetzer, 2015; van Steensel and Belmont, 2017). Furthermore, the subnuclear position of individual genes and their inter-chromosomal proximity can change depending on their expression status, suggesting that the spatial organization of genomes within the nucleus is dynamic, actively controlled and linked to expression (Edelman and Fraser, 2012; Egecioglu and Brickner, 2011; Eskiw et al., 2010; Takizawa et al., 2008).

What information determines this spatial organization? If sequence-specific DNA-binding transcription factors (TFs) impact the positioning of their target genes, then the spatial organization of genomes could be genetically encoded through their binding sites (Fraser and Bickmore, 2007). Supporting this idea, targeting genes to nuclear speckles (Hu et al., 2010) or the lamina (Harr et al., 2015; Zullo et al., 2012) and inter-chromosomal clustering (Haeusler et al., 2008; Noma et al., 2006; Spilianakis et al., 2005; Apostolou and Thanos, 2008; Schoenfelder et al., 2010) requires either *cis*-acting DNA elements or TFs. However, because TFs are multifunctional, it is difficult to distinguish between the effects of TFs and the effects of transcription on gene positioning.

The targeting of genes to the yeast NPC upon activation is also dependent on TFs that bind to their promoters but is independent of RNA polymerase II transcription (Brickner et al., 2007; Brickner et al., 2016; Schmid et al., 2006). TFs may play a similar role in recruiting nuclear pore proteins to genes in metazoan organisms (Buchwalter et al., 2014; Liang et al., 2013; Pascual-Garcia et al., 2014; Raices et al., 2017). Importantly, when inserted at an ectopic location, these TF binding sites function as "DNA zip codes," targeting the ectopic locus to the NPC and stimulating inter-chromosomal clustering in a TF-dependent manner (Ahmed et al., 2010; Brickner et al., 2012, 2016; Light et al., 2010; Randise-Hinchliff et al., 2016; Kim et al., 2017; Randise-Hinchliff et al., 2016). Studies with a handful of inducible genes have identified five TFs from distinct families and with distinct mechanisms of regulation that promote interaction with the NPC and, in some cases, induce inter-chromosomal clustering (Put3, Sfl1, Gcn4, Ste12, and Cbf1; Randise-Hinchliff and Brickner, 2016). However, dissection of the functional DNA zip codes in the promoters of these inducible genes also reveals that several other TFs (e.g., Ino2, Mig1, and Gal4) do not impact gene positioning. Thus, some, but not all, TFs control gene positioning and inter-chromosomal clustering, and it is unclear how many fall into each class.

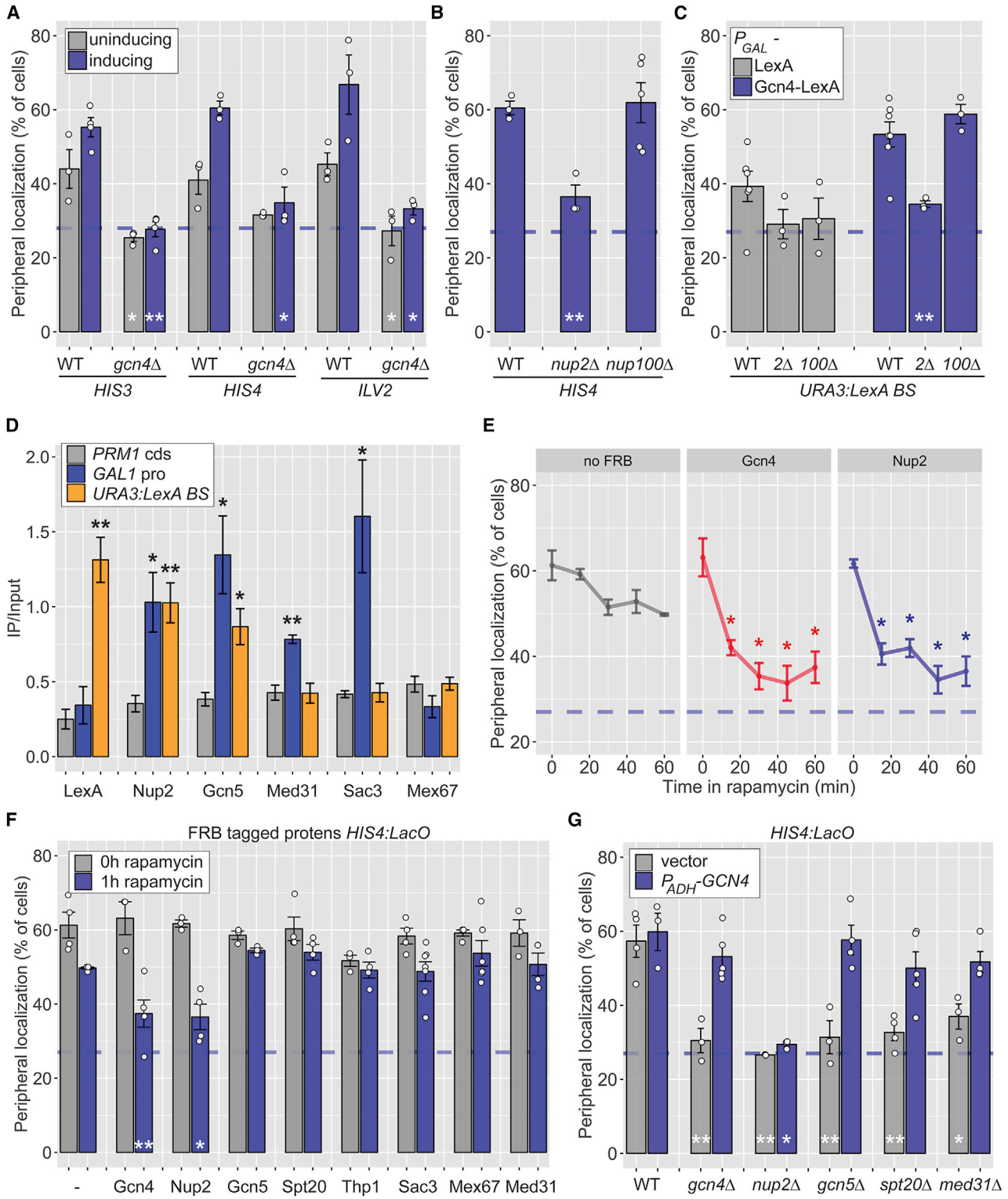

Figure 1. Gcn4-Mediated Targeting to the Nuclear Pore Complex

(A) Wild type or *gcn4Δ* grown either ± histidine (*HIS3* and *HIS4*) or ± leucine (*ILV2*).

(B) Wild type, *nup2Δ*, and *nup100Δ HIS4:LacO* in −histidine.

(C) Wild type, *nup2Δ*, and *nup100Δ URA3:LexABS-LacO* with P_{GAL}-*LexA* or P_{GAL}-*GCN4-LexA* in galactose.

(D) ChIP from P_{GAL}-*GCN4-LexA* + *URA3:LexA BS* against GFP-tagged proteins. Mean recovery of *PRM1*, *GAL1* promoter, and *URA3*, quantified by real-time quantitative PCR (error bars = SEM).

(legend continued on next page)

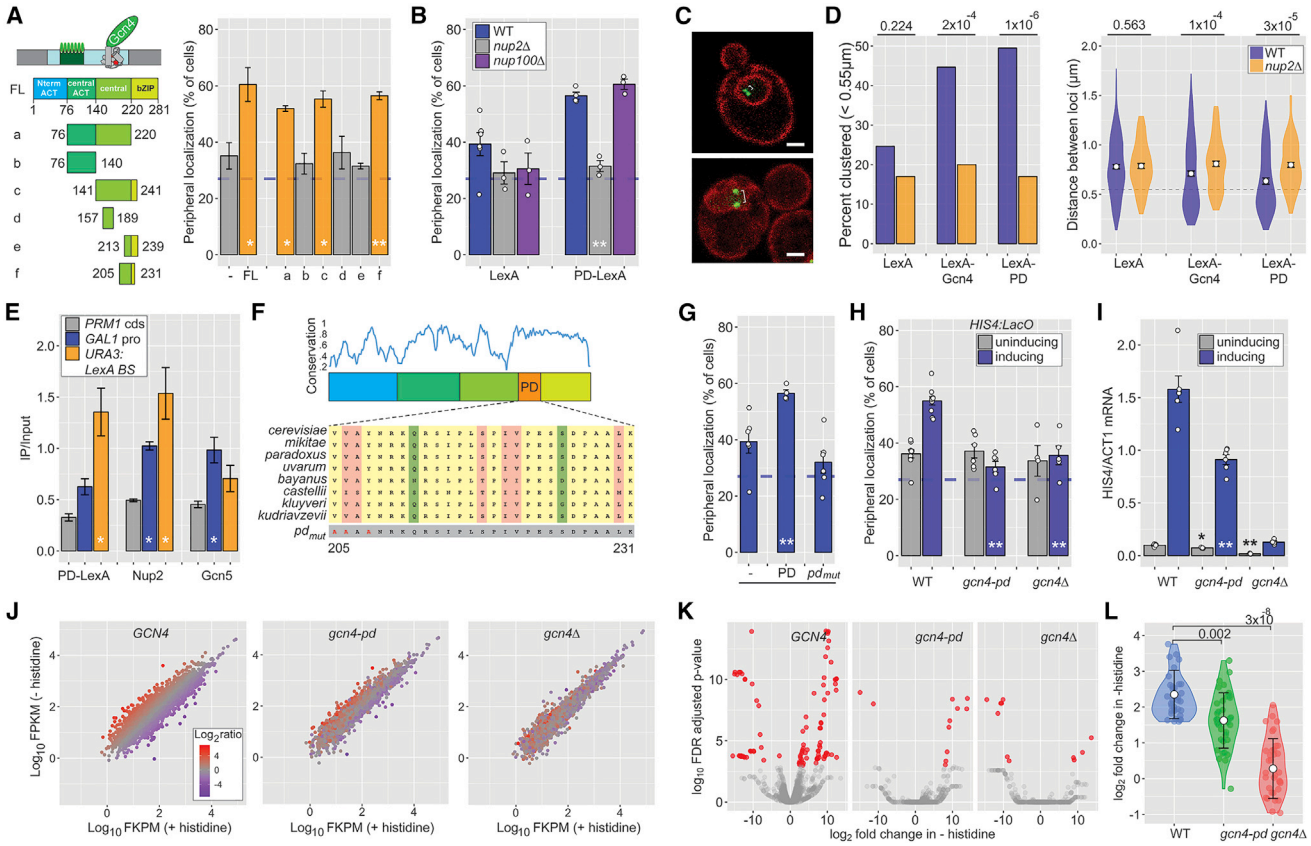

Figure 2. A Positioning Domain within Gcn4

(A) Left: schematic of Gcn4 and fragments fused to the LexA DNA-binding domain in the *URA3:LexA BS-LacO* strain (right; −, LexA alone; peripheral = orange).

(B) Localization of *URA3:LexABS-LacO* in wild type, *nup2Δ*, or *nup100Δ* with either LexA or PD_{GCN4}-LexA (in panels A, B, G & H, error bars = SEM).

(C) Confocal micrographs of diploid cells having both alleles of *URA3* tagged with the LacO array; scale bars = 1μm; distance between alleles was measured as indicated.

(D) The fraction of cells in which the distances were ≤ 0.55 μm (bar graphs, left) and the distribution of distances (violin plots, right; white circle = mean ± SEM) are plotted (n ≥ 100).

(E) ChIP for PD_{GCN4}-LexA, Nup2, or Gcn5; mean recovery of *GAL1-10* promoter, *PRM1*, or the LexA-binding site ± SEM.

(F) Location and conservation of the positioning domain (PD_{GCN4}) and a mutation that inactivates the PD_{GCN4} (pd_{mut}).

(G) Localization of *URA3:LexA BS* with LexA, PD_{GCN4}-LexA, or pd_{mut}-LexA.

(H) *HIS4* localization in wild type, *gcn4-pd*, and *gcn4Δ*.

(I) *HIS4* mRNA levels from wild type, *gcn4-pd*, and *gcn4Δ* ± histidine, relative to *ACT1*.

(J) Scatterplots of wild type, *gcn4-pd*, and *gcn4Δ* RNA sequencing (RNA-seq) $\log_{10}$ fragments per kilobase of exon per million reads mapped (FKPM) ± histidine. Heatmap: $\log_2$ (−histidine:+histidine) ratio in wild-type cells.

(K) Volcano plots of $\log_2$ (fold change) versus $\log_{10}$ of the false discovery rate (FDR)-adjusted p value for each transcript in each strain ± histidine. Red, >4-fold induced; FDR < 0.1%.

(L) Fold induction of Gcn4 target genes, with mean ± SD. * $p < 0.05$; ** $p < 0.01$.

To dissect the roles of TFs in controlling gene positioning from their roles in chromatin modification and transcription, we tested whether the recruitment of co-activators such as SAGA (Spt/Ada/Gcn5L histone acetyltransferase) and Mediator or mRNA export factors such as TREX-2 and Mex67 by the Gcn4 TF serves to bridge the interaction between Gcn4 and the NPC. Genetic and biochemical experiments argue that these factors, while genetically required for Gcn4-mediated targeting to the nuclear periphery, do not serve to bridge the interaction with the NPC. In contrast, Gcn4 and the NPC protein Nup2 play a direct role, and a 27 amino acid positioning domain (PD_{GCN4}) within Gcn4 is both necessary and sufficient to promote Nup2 recruitment, peripheral localization, and inter-chromosomal clustering.

(E) *HIS4-LacO* localization upon Anchor Away of Gcn4 or Nup2.

(F) *HIS4-LacO* localization upon Anchor Away of indicated factors for 1 h (−, no FRB control).

(G) *HIS4-LacO* localization in the indicated strains with or without overexpression of *GCN4*. Statistical analysis in STAR Methods; *p < 0.05; **p < 0.01.

(A–C, E, and F) Mean percent peripheral ± SEM is plotted from ≥ 3 biological replicates of 30–50 cells each (white dots). Blue, hatched line: expected percent of cells with genes ≤ 0.1 μm from the membrane (~27%; Figure S1A).

To explore the scope of TF-mediated gene positioning to the nuclear periphery, we screened 187 yeast-DNA-binding proteins for their ability to target a chromosomal site to the nuclear periphery. Tethering of most yeast TFs (~ 65%) causes targeting to the nuclear periphery. The NPC is the major site to which TFs target, and targeting can occur by at least two distinct mechanisms. Validating the results of the screen, endogenous target genes of several positives exhibit TF- and Nup2-dependent localization to the periphery and inter-chromosomal clustering. TFs from every family, including activators, repressors, and chromatin factors, mediated targeting to the NPC, arguing against a simple model for NPC function in transcriptional regulation. Thus, yeast TFs, together with nuclear pore proteins, play a critical role in controlling the spatial organization of the yeast genome.

RESULTS AND DISCUSSION

Gcn4 and Nup2 Play Direct Roles in Mediating Peripheral Gene Positioning

As a model for TF-mediated targeting to the nuclear periphery in budding yeast, we focused on Gcn4. To monitor interaction with the NPC, we tagged loci of interest with an array of 128 Lac operators (LacO array; Robinett et al., 1996) and expressed GFP-LacI and a fluorescent membrane marker for the endoplasmic reticulum and nuclear membrane, allowing the locus of interest to be scored for colocalization with the nuclear envelope by confocal microscopy (Brickner and Walter, 2004; Egecioglu et al., 2014). Simulation of random positions within the yeast nucleus showed that a position should be within 100 nm of the nuclear envelope in ~27% of the population (Figure S1A, hatched blue line throughout). We observe that genes that localize in the nucleoplasm colocalize with the nuclear envelope in 25%–30% of the cells in a population, while interaction with the NPC leads to an increase in colocalization to ~50%–65% of the cells (Brickner and Walter, 2004).

Peripheral localization of Gcn4 target genes reflects Gcn4 protein levels and promoter occupancy (Randise-Hinchliff et al., 2016). *HIS3*, *HIS4*, and *ILV2* show low but detectable peripheral localization (40%–45%) in cells grown with amino acids, and starvation for amino acids induces an increase in Gcn4 protein translation and upregulation of its target genes (Hinnebusch, 1997; Hinnebusch and Fink, 1983; Lucchini et al., 1984; Mueller et al., 1987), leading to an increase in peripheral localization of these genes to ~60% of the population (Figure 1A). Peripheral localization requires Gcn4 and the nuclear pore protein Nup2 (Figures 1A and 1B). In contrast, loss of the nuclear pore protein Nup100—a factor that to date has only been associated with Sfl1-mediated targeting of *INO1* to the NPC—did not affect *HIS4* localization (Figure 1B). Thus, repositioning of Gcn4 target genes to the nuclear periphery requires Gcn4 and Nup2 but not Nup100.

Gcn4 binding to a chromosomal site is also sufficient to cause peripheral localization: tethering Gcn4 to the nucleoplasmic locus *URA3* using the LexA DNA-binding domain (DBD) leads to peripheral localization (Randise-Hinchliff et al., 2016). Peripheral localization of *URA3:LexABS* requires Nup2, but not Nup100, suggesting that tethering recapitulates Gcn4-mediated targeting (Figure 1C).

Although mRNA production is not required for peripheral localization, many other factors such as transcriptional co-activators, such as the SAGA histone acetyltransferase and Mediator, and mRNA export factors, such as TREX-2 and Mex67, are required for targeting of certain genes to the nuclear periphery (Ahmed et al., 2010; Cabal et al., 2006; Dieppois et al., 2006; Luthra et al., 2007; Schneider et al., 2015; Dultz et al., 2016). These factors physically interact with the NPC, suggesting the hypothesis that recruitment of these factors to specific chromosomal sites by TFs could bridge the interaction with the NPC. We tested three predictions of this hypothesis: (1) such factors should be recruited to an ectopic site to which the TF is tethered, (2) conditional inactivation of such factors should lead to rapid loss of peripheral localization, and (3) such genes should function downstream of the TF in targeting to the periphery.

To test the first prediction, we asked if tethering of Gcn4 to *URA3* using the LexA-binding site is sufficient to recruit Nup2, SAGA (Gcn5), Mediator (Med31), TREX2 (Sac3), or Mex67. In a strain having *URA3:LexABS* and expressing Gcn4-LexA under the control of the *GAL1-10* promoter, we performed chromatin immunoprecipitation (ChIP) against LexA (Gcn4) or against GFP-tagged Nup2, Gcn5, Med31, Sac3, and Mex67. The recovery of *URA3:LexABS*, a negative control (nucleoplasmic, repressed *PRM1*) and a positive control (active NPC-interacting *GAL1-10* promoter; Casolari et al., 2004) was quantified by qPCR (Figure 1D). While Nup2, SAGA, Mediator, and TREX-2 were all recruited to the *GAL1-10* promoter, only Nup2 and SAGA were recruited to *URA3:LexABS* (Figure 1D). Mex67 association was not detected at either site. Thus, while tethering of Gcn4 to a non-promoter locus causes peripheral localization, it is not sufficient to recruit Mediator, TREX2, or Mex67.

To conditionally inactivate these factors, we utilized Anchor Away to remove them from the nucleus (D'Urso et al., 2016; Haruki et al., 2008). Anchor Away of Gcn4-FRB or Nup2-FRB led to relocalization of *HIS4* to the nucleoplasm within 15–30 min (Figure 1E). However, Anchor Away of SAGA (Gcn5 and Spt20), TREX-2 (Thp1 and Sac3), Mediator (Med31), or Mex67 for >1 h did not significantly reduce *HIS4* localization at the nuclear periphery, suggesting that they are not bridging the interaction with the NPC (Figure 1F). After extended Anchor Away of these factors (5 h), peripheral localization was disrupted, recapitulating the null phenotype (Figure S1B).

As Gcn4 target gene localization to the nuclear periphery reflects Gcn4 levels and occupancy of its binding sites (Figure 1A), we next tested if over-production of Gcn4 affects the phenotype in null mutant strains lacking factors involved in transcription or mRNA export. Over-production of Gcn4 (under the control of the *ADH1* promoter and lacking the upstream open reading frames; Mueller et al., 1987; Randise-Hinchliff et al., 2016) complemented the *gcn4Δ* phenotype but had no effect on the *nup2Δ* phenotype (Figure 1G). This confirms that Nup2 functions downstream of Gcn4 in targeting of *HIS4* to the nuclear periphery.

In contrast, over-production of Gcn4 suppressed the defect in *HIS4* targeting to the nuclear periphery in the SAGA mutants *gcn5Δ* and *spt20Δ* and the Mediator mutant *med31Δ* (Figure 1G). In other words, while they are genetically required for peripheral targeting of *HIS4*, their function was bypassed by increasing the occupancy of Gcn4 at the *HIS4* promoter. Therefore, while Gcn4

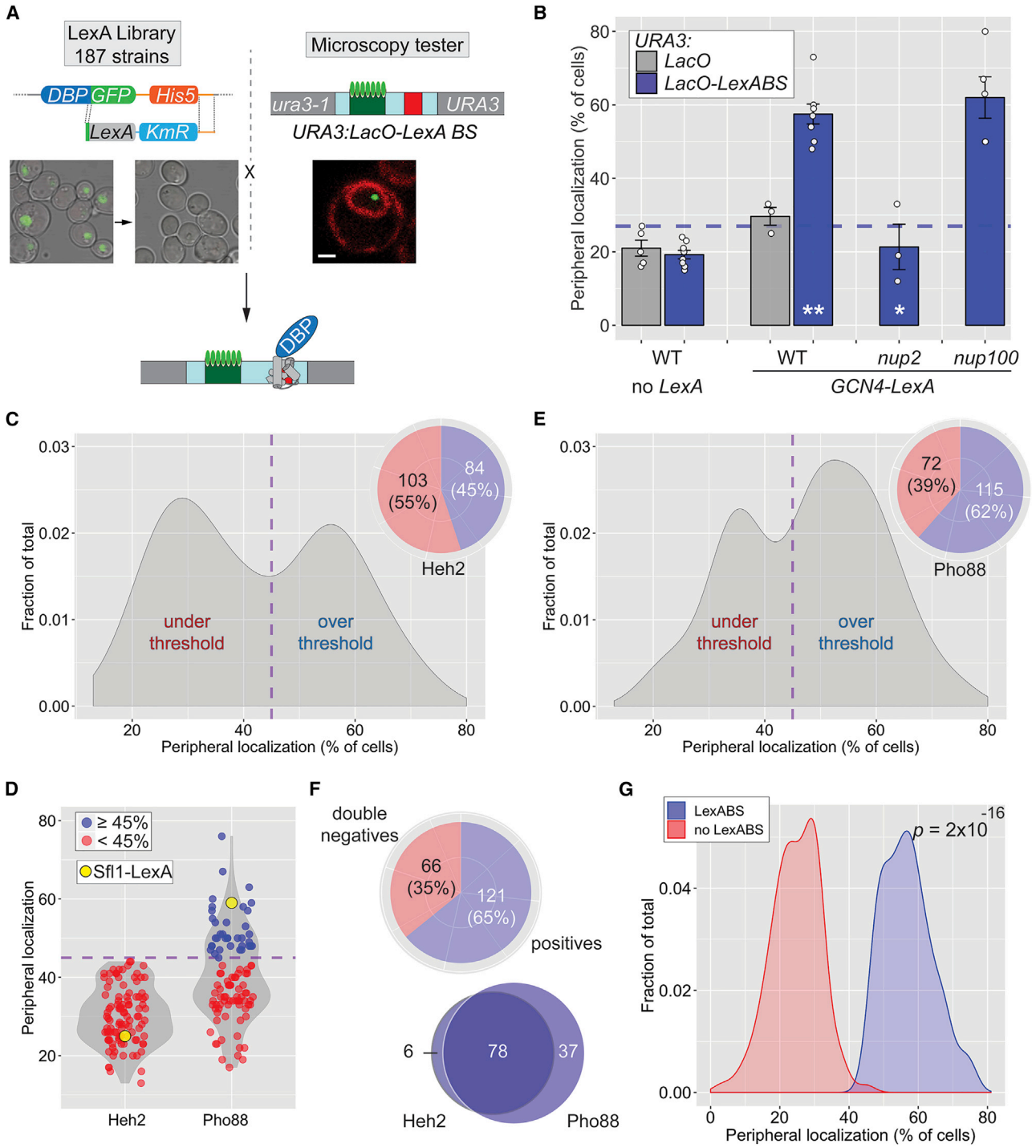

Figure 3. Tethering of Yeast Transcription Factors Mediates Repositioning to the Nuclear Periphery

(A) Schematic for the LexA-tethering screen.

(B) Peripheral localization of *URA3* ± LexA BS and ± Gcn4-LexA in wild type, *nup2*, or *nup100*. Error bars = SEM; *p < 0.05; **p < 0.01.

(C and E) Summary of 187 DNA-binding proteins (DBPs) using either the ER/nuclear envelope marker made from the Heh2 (C; Egecioglu et al., 2014) or the Pho88-mCherry marker (E; D'Urso et al., 2016; Sood et al., 2017). Bimodal distributions were modeled (Figure S3B) for two populations having means of ~30% ± 7.6% and ~57% ± 7.6%. Threshold for positives = 45% (1.96 SDs > lower mean; purple hatched line). Inset: summary of the fraction of DBPs above and below the threshold.

(D) Results for DBPs that were below the threshold from the Heh2 screen. Red = negatives; blue = positives. Sfl1 highlighted in yellow.

(F) Top: summary of DBPs below the threshold in both screens (double negatives) or above the threshold in either screen. Bottom: overlap in positives.

(G) Heh2 positives and Pho88-specific positives (blue) were retested by crossing to a microscopy tester strain lacking the LexA-binding site (red). p Value from Student's t test.

and Nup2 play direct roles in peripheral targeting of *HIS4*, SAGA, Mediator, TREX-2, and Mex67 likely play indirect roles.

Gcn4 Has a Positioning Domain

To further define Gcn4-mediated targeting to the nuclear periphery, we exploited the LexA-tethering system to identify the portion of Gcn4 responsible for this activity (Figure 2A). A 27-amino-acid fragment from Gcn4 (amino acids 205–231) is sufficient to target *URA3:LexABS* to the nuclear periphery (Figure 2A). Targeting is dependent on Nup2, but not Nup100 (Figure 2B), suggesting that this "positioning domain" (PD_{GCN4}) mediates targeting by the same mechanism as full-length Gcn4.

Genes that share DNA zip codes can undergo TF- and nuclear pore-dependent inter-allelic and inter-genic clustering (Brickner et al., 2012, 2016; Kim et al., 2017; Randise-Hinchliff et al., 2016). Targeting of *HIS4* to the nuclear periphery leads to inter-allelic clustering (Randise-Hinchliff et al., 2016), so we also tested if tethering of the PD_{GCN4} in diploid strains having two copies of *URA3:LexABS* was sufficient to induce inter-allelic clustering (Figures 2C and 2D). Based on the fraction of the population in which the two alleles were $\leq$0.55 μm apart (Figure 2D, left panel; Fisher's exact test), and the shape of the distribution of distances between the two alleles in the population (Figure 2D, right panels; two-sided Kolmogorov-Smirnov test), tethering of either Gcn4-LexA or PD_{GCN4}-LexA resulted in a significant increase in Nup2-dependent clustering (Figure 2D). Thus, the PD_{GCN4} is sufficient to induce both localization at the nuclear periphery and inter-allelic clustering.

ChIP against either Nup2 or SAGA in strains expressing PD_{GCN4}-LexA revealed that while the PD_{GCN4} is sufficient to recruit Nup2 to *URA3:LexABS*, it is not sufficient to recruit SAGA (Figure 2E). Therefore, PD_{GCN4}-mediated targeting to the nuclear periphery correlates with a physical interaction with the NPC but does not lead to recruitment of other factors associated with transcription.

The PD_{GCN4} is within the central domain of Gcn4, distinct from its activation domains (Drysdale et al., 1995; Hope et al., 1988; Hope and Struhl, 1986; Figure 2A). This portion of Gcn4 is highly conserved among Gcn4 homologs in *Saccharomyces* species (Figure 2F). Introducing mutations into PD_{GCN4}-LexA, we identified a mutation replacing three conserved amino acids with alanine ($V_{205}A\ V_{206}A\ Y_{208}A$; pd_{mut}; Figure S2A) that disrupted targeting of *URA3:LexABS* (Figure 2G). Mutation of the PD in endogenous *GCN4* (*gcn4-pd*) disrupted targeting of *HIS4* to the nuclear periphery (Figure 2H). The *pd* mutation does not affect either Gcn4 protein levels or DNA binding: wild-type Gcn4 and Gcn4-pd occupancy of the *HIS4* promoter was indistinguishable (Figure S2B). Thus, the positioning domain controls targeting to the nuclear periphery and inter-chromosomal clustering.

The *pd* mutation also led to a significant decrease in the expression of *HIS4* upon histidine starvation (Figure 2I). Next-generation sequencing of mRNA from cells grown ± histidine revealed that direct targets of Gcn4 were strongly enriched among mRNAs upregulated $\geq$ 3-fold by histidine starvation ($p = 9 \times 10^{-4}$, Fisher's exact test; direct targets from Rawal et al., [2018]). However, both the *gcn4Δ* and *gcn4-pd* mutants showed general derangement in the transcriptional response to histidine starvation (Figure 2J) and fewer significant expression changes (Figure 2K). In both measures, the *gcn4-pd* mutant exhibited a less severe phenotype than the null mutant. Gcn4 targets that were upregulated $\geq$ 3-fold upon histidine starvation in the wild-type cells (n = 36) were less strongly induced in the *gcn4-pd* mutant (Figure 2L), suggesting that the PD_{GCN4} is essential for both Gcn4-mediated peripheral targeting and full Gcn4-dependent transcription.

A Tethering Screen to Assess the Role of Transcription Factors in Controlling Gene Positioning to the Nuclear Periphery

Our work with Gcn4 suggests that TFs play a direct and specific role in controlling the interaction with the NPC and inter-chromosomal clustering. To explore this function of TFs globally, we exploited the LexA-tethering system to test 187 yeast-DNA-binding proteins for their ability to target the *URA3* locus to the nuclear periphery (Figure 3A; Table S1). Because these DNA-binding proteins are strongly enriched for regulation of transcription (169 of 187 factors; GO:0006355 enrichment $p = 5 \times 10^{-133}$; Table S2), we refer to them as TFs, although they include proteins that both activate and repress transcription, as well as factors involved in chromatin-based regulation (Table S1). Endogenous genes encoding these TFs were tagged with the LexA DBD by replacing the C-terminal GFP-tag in strains from the yeast GFP strain collection (Huh et al., 2003; Figure 3A, left). The re-tagged strains were crossed against a strain with *URA3:LexABS-LacO* and expressing GFP-LacI and a fluorescent marker for the nuclear envelope (Figure 3A, right). This tethering strategy faithfully recapitulated Gcn4-mediated targeting to the NPC (Figure 3B). Because some TFs are sensitive to the fluorescent ER marker (D'Urso et al., 2016), we performed two parallel screens with either an overexpressed fusion protein derived from Heh2 (Meinema et al., 2011; Egecioglu et al., 2014) or with a tagged endogenous ER membrane protein, Pho88 (D'Urso et al., 2016; Sood et al., 2017).

Peripheral localization of *URA3:LexABS* was scored in diploid strains expressing LexA-tagged TFs by confocal microscopy. For each strain, $\geq$30 cells were measured, which simulations suggested would be sufficient to distinguish peripheral and nucleoplasmic localization patterns (Figure S3A). The peripheral localization of *URA3:LexABS* from this collection of strains exhibited a bimodal distribution (Figures 3C and 3E; Tables S3 and S4), which we modeled as two different populations, one with a mean of 30% ± 8% peripheral and the other with a mean of 57% ± 8% peripheral (Figure S3B). This provided a conservative threshold of 45% separating the two populations (~2 standard deviations above the lower mean; purple hatched line). Using this threshold, 84 of the TFs tested with Heh2 (~45%; Figure 3C) and 115 of the TFs tested with Pho88 (~62%; Figure 3E) targeted *URA3:LexABS* to the nuclear periphery. The positives from the Pho88 screen included several that had been negatives in the Heh2 screen (Figure 3D).

Combining the results from both screens, 121 TFs (65%) were above the threshold in at least one screen and 66 (34%) were below the threshold in both (Figure 3F). Rescreening the positives in a strain without the LexA-binding site confirmed that peripheral targeting required tethering (Figure 3G; Table S5). We also explored the frequency of false positives by fusing the LexA DBD to a collection of 13 cytoplasmic enzymes or nuclear

proteins that do not bind DNA (Figure S3G; Table S4). Only one showed marginal targeting (45% peripheral), suggesting that tethering random proteins to chromatin does not lead to repositioning, supporting the conclusion that tethering of a majority of yeast TFs is sufficient to reposition an ectopic site to the nuclear periphery.

While tethering does not establish that the TFs directly interact with the NPC, the prevalence of positives suggests that interaction with the NPC is associated with different types of transcription (constitutive and inducible) and different types of regulation (activation, repression, and chromatin). The positives included members of all of the families of yeast TFs (Figure S3C), activators, repressors, and chromatin regulators (Figure S3D). There was no difference in mean protein abundance of the TFs that were positives or negatives ($p = 0.33$, Student's t test; Figure S3E). Likewise, the median mRNA abundance of the targets of the positive TFs was comparable to the abundance of the targets of the negative TFs (Figure S3F). These results suggest that the positive TFs from the screen are a representative sample of all yeast TFs and do not possess obviously different properties.

The significance of the negatives from the screens is unclear. Among the negatives are TFs that do not mediate targeting to the periphery such as Ino2 and Gal4 (Ahmed et al., 2010; Brickner et al., 2016; Randise-Hinchliff et al., 2016). However, we also observed examples of false negatives in the screen, likely because of intolerance of C-terminal tagging or regulated function. For example, two TFs that are capable of mediating targeting to the nuclear periphery scored as negatives: Put3, perhaps because it is non-functional when C-terminally tagged (Brickner et al., 2012), and Ste12, presumably because it is only functional upon pheromone treatment (Randise-Hinchliff et al., 2016). Consistent with this caveat, targeting of *URA3:LexABS* to the nuclear periphery by several TFs that are regulated by DNA damage was induced by treatment with hydroxyurea (Figure S3H). Therefore, the fraction of TFs capable of mediating peripheral localization is greater than 65%, and classification of TFs as unable to mediate peripheral localization should be considered provisional.

TFs Mediate Targeting to the NPC by Two Different Pathways

Several possible mechanisms could lead to positioning to the nuclear periphery. TFs could promote interaction with the NPC, the nuclear envelope, the spindle pole body, or other structures at the nuclear periphery. However, comparison of the overlap between TF target genes (https://yeastmine.yeastgenome.org/yeastmine/begin.do) and nuclear-pore-protein-binding sites from ChIP-chip (NPC basket proteins Nup60, Nup2, Mlp1, and Mlp2 [Casolari et al., 2005, 2004] or Nup157 and Nup170 [Van de Vosse et al., 2013]) revealed that the overlap was stronger for target genes regulated by positives than for target genes regulated by negatives (Figures 4A and 4B). The most significant overlap was between the Nup binding sites and the targets of TFs that regulate transcription of glucose metabolism genes (Gcr1 and Tup1), ribosome protein genes (Sfp1, Fhl1, and Ifh1), or both (Rap1 and Hsf1; Figure 4B). All of these TFs were positives in our screens, and individual target genes of Gcr1, Tup1, Rap1, and Hsf1 localize at the nuclear periphery or show inter-chromosomal clustering (Chowdhary et al., 2017; Sarma et al., 2007; Sood et al., 2017; Taddei et al., 2006). Thus, there is a correlation between positives in the screen and TFs that regulate the genes that physically interact with the NPC.

To identify those TFs that mediate targeting to the NPC, we used CRISPR-Cas9 (as in Figure 3B) to create null mutations in *NUP2* and *NUP100* in the positive diploids from the primary screen. To date, Nup2 is generally required for targeting to the NPC, while Nup100 has only been shown to be required for Sfl1-mediated targeting (Ahmed et al., 2010; Brickner et al., 2007; Cabal et al., 2006; D'Urso et al., 2016; Light et al., 2010). Inactivation of Nup2 resulted in loss of peripheral localization in >97% of the strains (Figure 4C; Table S6), confirming that the NPC is the major site to which tethered TFs target *URA3*:*LexABS* and that essentially all of the TFs require Nup2. This mutation had no effect on the localization of the TFs to the nucleus (Figure S4). In contrast, 63% of the positives require Nup100, and the remaining 37% are Nup100 independent (Figure 4C; Table S6). For example, Sfl1, Fhl1, and Sfp1 were dependent on both Nup2 and Nup100, while Gcn4 and Tup1 were dependent on Nup2, but not Nup100 (Figure 4C). This suggests that TFs mediate targeting to the NPC by two pathways, one that is Nup100 dependent and another that is Nup100 independent. Contrary to our expectations from studies of a handful of inducible genes, more TFs require both Nup2 and Nup100, suggesting that this is the more common pathway.

Endogenous Target Genes Localize at the Nuclear Periphery and Exhibit TF- and Nup2-Dependent Inter-chromosomal Clustering

To confirm that the positives from the tethering screen reflect TF-dependent targeting of target genes, we tagged several endogenous genes that are regulated by the positives with the LacO array. Peripheral localization of these genes was observed after induction by either glucose starvation or heat shock (Figure 4D; *URA3* is a negative control under these conditions). Furthermore, targeting of Hsf1 targets *SSA2* and *SSA4* to the nuclear periphery was Nup2-dependent (Figure 4E). Thus, the screen revealed TFs that mediate targeting to the NPC.

The screen also identified TFs that regulate constitutively expressed genes, such as the Forkhead-like TF Fhl1, which binds as a heterodimer with Ifh1 to regulate ribosomal protein gene transcription (Rudra et al., 2005). While ribosomal protein genes show Nup170 association over both their promoters and coding sequences, occupancy of Fhl1-Ifh1 was correlated with Nup170 promoter association (Figure S5; Reja et al., 2015; Van de Vosse et al., 2013). Thus, ribosomal protein genes likely interact with the NPC, and the promoter interactions may be mediated by Fhl1/Ifh1.

We confirmed that three ribosomal protein genes (*RPS0A*, *RPS1B*, and *RPS6A*) physically interact with Nup2-TAP by ChIP (Figure S5G) and localize at the nuclear periphery (Figure 5A). DNA fluorescence *in situ* hybridization (FISH) against *RPS0A* also showed peripheral localization in a strain lacking the LacO array (Figure S5F). Anchor Away to remove Nup2 or Fhl1 from the nucleus led to loss of peripheral localization within 30–60 min (Figure 5B), correlating well with the depletion of Fhl1 from the nucleus (Figure S5H). Furthermore, the peripheral localization of *ACT1* was unaffected by depletion of Fhl1, confirming

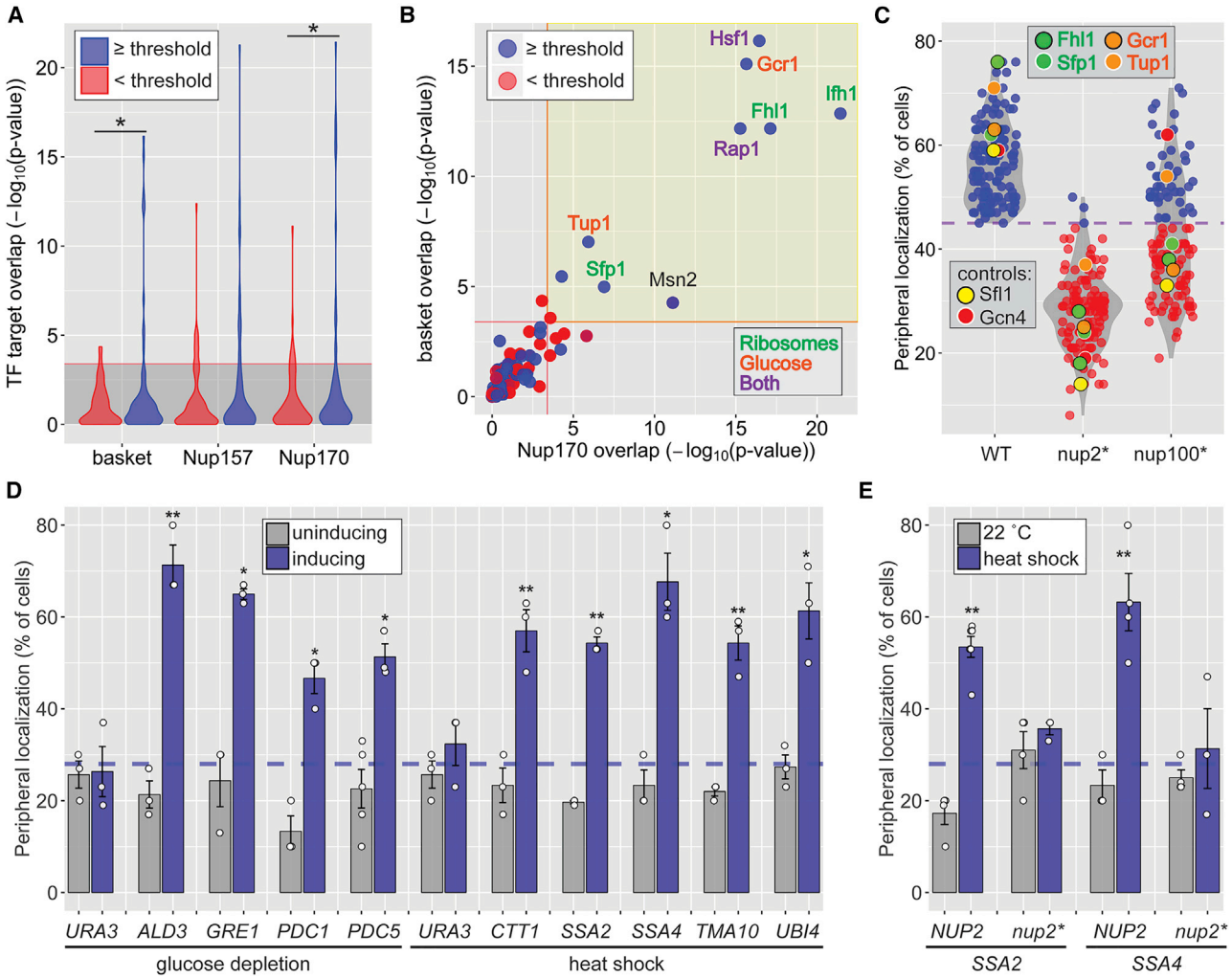

Figure 4. TF-Dependent Targeting to NPC Occurs through Two Different Pathways

(A and B) Overlap between targets of TFs and chromosomal sites that interact with the NPC basket (Nup2, Nup60, Mlp1, and Mlp2; Casolari et al., 2004) or the Nup157 and Nup170 (Van de Vosse et al., 2013) was compared with the Fisher's test, giving a distribution of $-\log_{10}$ p values (A); to correct for multiple hypothesis testing, the significance threshold is $p = 4 \times 10^{-4}$ (red line).

(B) Highlight of overlap between the NPC basket/Nup170 interactions and targets of individual TFs.

(C) *NUP2* or *NUP100* were disrupted in the diploid strain positives. Results for individual TFs (Fhl1, Sfp1, Gcr1, and Tup1) and controls (Gcn4 and Sfl1) are highlighted. Both Heh2 and Pho88 positives were tested for Fhl1.

(D) Localization of endogenous genes in SDC (synthetic dextrose complete; uninducing), SEGC (synthetic ethanol-glycerol complete; glucose-regulated inducing), 22°C (heat shock uninducing), or 37°C (heat shock inducing). (E) Localization in wild type or *nup2** mutant strains. Error bars = SEM; * $p < 0.05$; ** $p < 0.01$.

that this effect is specific (Figure 5B). Therefore, endogenous Fhl1/Ifh1 target genes are positioned at the nuclear periphery in a Fhl1-Ifh1- and Nup2-dependent manner.

We also measured inter-allelic and inter-genic distances in diploid strains tagged for *RPS0A* and *RPS6A* to test if Fhl1/Ifh1 target genes exhibit this behavior. Simulation (Figure S1A) predicts that 11.9% of the population would be $\leq$ 0.55 μm by chance, with a mean distance of 1.02 μm, similar to the nucleoplasmic gene *URA3* (Brickner et al., 2012, 2016). In contrast, we observed a clear bimodal distribution with significantly higher inter-allelic clustering of *RPS0A* ($p = 2 \times 10^{-8}$; two-sided Kolmogorov-Smirnov test of distributions) and *RPS6A* ($p = 3 \times 10^{-9}$) and inter-genic clustering between *RPS0A* and *RPS6A* ($p = 5 \times 10^{-6}$; Figure 5D). The *RPS1B* gene showed neither inter-allelic nor inter-genic clustering (data not shown). Clustering of *RPS0A* and *RPS6A* was lost in strains lacking Nup2 (Figure 5C) or in strains in which Fhl1 was inactivated by Anchor Away (Figure 5D). Thus, these target genes show Nup2- and Fhl1-dependent inter-chromosomal clustering.

Conclusions

Based on our work with Gcn4, we propose that TFs directly control gene positioning through positioning domains, while other factors associated with transcription and mRNA export are not directly involved in tethering genes to the NPC. We have identified a peptide that controls both gene positioning and

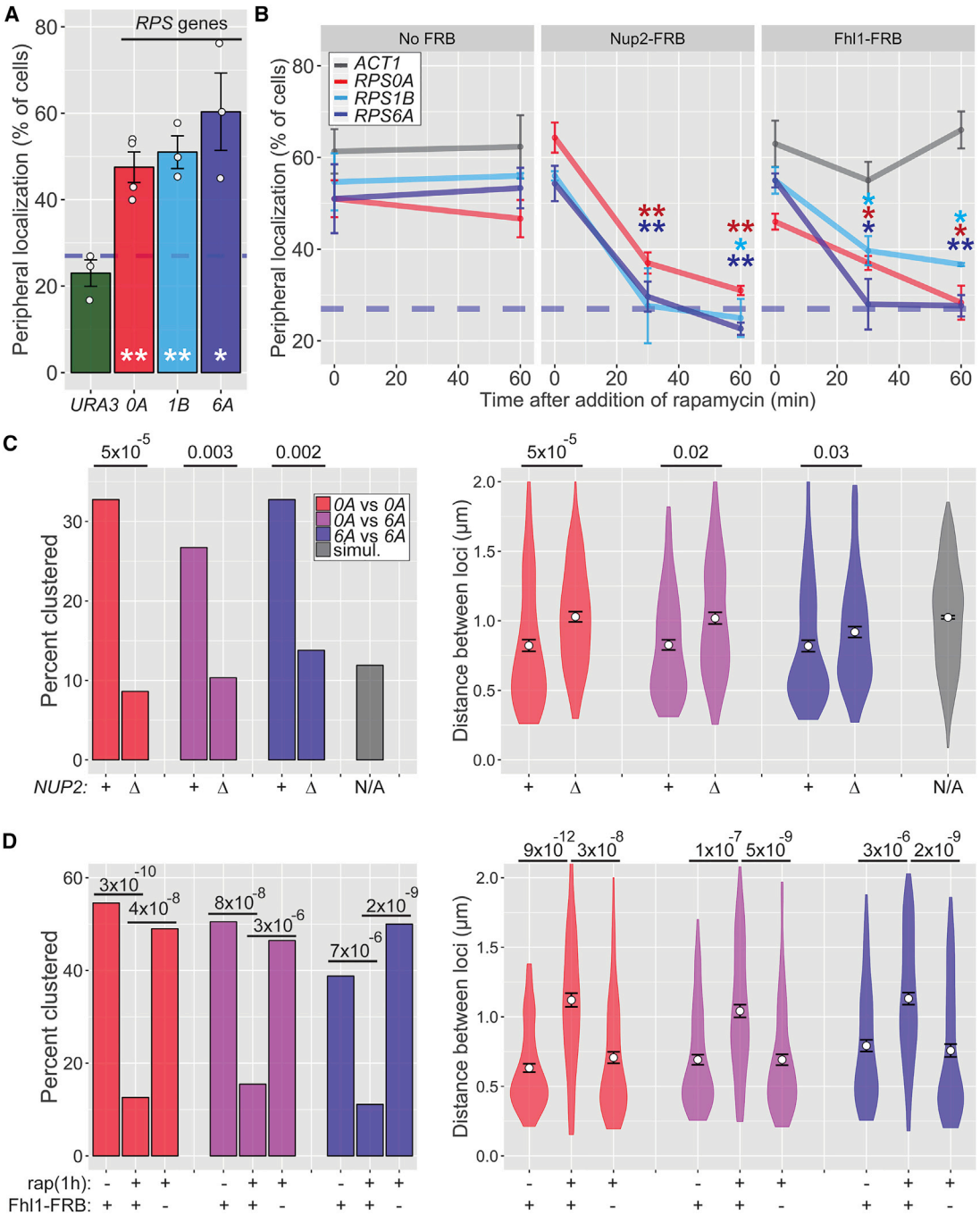

Figure 5. Localization and Inter-chromosomal Clustering of Endogenous Fhl1/Ifh1 Targets

(A) Localization of *URA3*, *RPS0A*, *RPS1B*, and *RPS6A*. Error bars = SEM.

(B) Localization of *ACT1*, *RPS0A*, *RPS1B*, and *RPS6A* upon Anchor Away of indicated proteins. Error bars = SEM.

(C and D) Diploid cells with both alleles of *RPS0A* (*0A* versus *0A*), both alleles of *RPS6A* (*6A* versus *6A*) or one allele of each (*0A* versus *6A*) tagged with the LacO. Fraction of cells in which the distances were ≤ 0.55 μm (bar graphs, left) and distribution of distances (right; white circle is the mean ± SEM). (C) Wild-type cells (+) versus *nup2* null (Δ). Gray: simulation of random distances. (D) Anchor Away of Fhl1. * $p < 0.05$; ** $p < 0.01$.

inter-chromosomal clustering, and this activity is separable from the other activities of TFs such as DNA binding and transcriptional regulation. Controlling positioning is apparently quite common. Our global gain-of-function screen revealed most yeast TFs can target an ectopic site to the NPC by (at least) two distinct pathways, Nup100 dependent and Nup100 independent. These TFs include activators, repressors, chromatin factors, etc. This striking result is both an important resource and highlights an

important conceptual point: the NPC may impact gene expression in many ways. This may explain why studies focused on different targets have suggested that the NPC promotes activation, repression, insulation, or RNA polymerase III transcription (Ahmed and Brickner, 2010; Brickner and Walter, 2004; Green et al., 2012; Ikegami and Lieb, 2013; Kalverda and Fornerod, 2010; Kalverda et al., 2010; Van de Vosse et al., 2013). Consistent with this notion, the effects of loss of Nup2 on transcription are more complex than the transcriptional effects of disrupting the interaction of single genes with the NPC, perhaps because of disparate effects (Dilworth et al., 2005).

This result also raises a number of interesting questions. Is the PD_{GCN4} a binding site for a factor that localizes at the nuclear periphery? The sensitivity of this motif to amino acid substitutions suggests that its function is due to specific recognition. The sequence of the PD_{GCN4} is not obviously related to the sequence of domains controlling gene positioning in other TFs (data not shown). This may not be surprising since the inter-chromosomal clustering of genes is both TF dependent and TF specific. Furthermore, positioning domains may be similar to TF activation domains, which share little obvious sequence identity but carry out essentially equivalent roles (Sigler, 1988; Warfield et al., 2014). Identification of the functional positioning domains from other TFs and determination of their molecular mechanism will reveal how TFs encode positioning and specific inter-chromosomal clustering.

STAR★METHODS

Detailed methods are provided in the online version of this paper and include the following:

- KEY RESOURCES TABLE
- CONTACT FOR REAGENT AND RESOURCE SHARING
- EXPERIMENTAL MODEL AND SUBJECT DETAILS
- METHOD DETAILS
  - Chemicals and Media and Growth Conditions
  - Yeast Strains, Plasmids and Molecular Biology
  - CRISPR/ Cas-9 Mutagenesis
  - Confocal Microscopy
  - Anchor Away
  - Chromatin Immunoprecipitation (ChIP)
  - RT-qPCR and RNAseq
  - DNA FISH
- QUANTIFICATION AND STATISTICAL ANALYSIS
- DATA AND SOFTWARE AVAILABILITY

SUPPLEMENTAL INFORMATION

Supplemental Information can be found online at https://doi.org/10.1016/j.devcel.2019.05.023.

ACKNOWLEDGMENTS

The authors thank members of the Brickner laboratory, Erik Andersen, and Alan Hinnebusch for helpful discussions and input. This work was supported by NIH R01 GM 080484 and R01 GM118712 (J.H.B.). A.D. was supported by NIH T32 GM008061; R.C., S.K., S.H.K., S.H., and R.W. were supported by Northwestern University undergraduate research fellowships. A.S. is supported by a JSPS Overseas postdoctoral fellowship from the Japanese Society for the Promotion of Science.

AUTHOR CONTRIBUTIONS

Conceptualization, J.H.B., D.G.B., and C.R.H.; Methodology, D.G.B., C.R.H., and J.M.L.; Software and Formal Statistical Analysis, J.H.B. and A.S.; Investigation, D.G.B., C.R.H., M.L.C., J.M.L., S.K., B.S., A.D., S.H.K., H.S., R.C., S.H., and R.W.; Writing, J.H.B., D.G.B., and C.R.H.; Visualization, J.H.B., D.G.B., and C.R.H.; Supervision, J.H.B. and D.G.B.; Project Administration, J.H.B.; Funding Acquisition, J.H.B.

DECLARATION OF INTERESTS

The authors declare no competing interests.

Received: October 15, 2018
Revised: April 18, 2019
Accepted: May 10, 2019
Published: June 17, 2019

WEB RESOURCES

YeastMine, https://yeastmine.yeastgenome.org/yeastmine/begin.do

REFERENCES

Ahmed, S., Brickner, D.G., Light, W.H., Cajigas, I., McDonough, M., Froyshteter, A.B., Volpe, T., and Brickner, J.H. (2010). DNA ZIP codes control an ancient mechanism for gene targeting to the nuclear periphery. Nat. Cell Biol. *12*, 111–118.

Ahmed, S., and Brickner, J.H. (2010). A role for DNA sequence in controlling the spatial organization of the genome. Nucleus *1*, 402–406.

Apostolou, E., and Thanos, D. (2008). Virus Infection Induces NF-kappaB-dependent interchromosomal associations mediating monoallelic IFN-beta gene expression. Cell *134*, 85–96.

Bickmore, W.A., and van Steensel, B. (2013). Genome architecture: domain organization of interphase chromosomes. Cell *152*, 1270–1284.

Brickner, D.G., Ahmed, S., Meldi, L., Thompson, A., Light, W., Young, M., Hickman, T.L., Chu, F., Fabre, E., and Brickner, J.H. (2012). Transcription factor binding to a DNA ZIP code controls interchromosomal clustering at the nuclear periphery. Dev. Cell *22*, 1234–1246.

Brickner, D.G., Cajigas, I., Fondufe-Mittendorf, Y., Ahmed, S., Lee, P.C., Widom, J., and Brickner, J.H. (2007). .S2AZ-mediated localization of genes at the nuclear periphery confers epigenetic memory of previous transcriptional state. PLoS Biol. *5*, e81.

Brickner, D.G., Light, W., and Brickner, J.H. (2010). Quantitative localization of chromosomal loci by immunofluorescence. Methods Enzymol. *470*, 569–580.

Brickner, D.G., Sood, V., Tutucci, E., Coukos, R., Viets, K., Singer, R.H., and Brickner, J.H. (2016). Subnuclear positioning and interchromosomal clustering of the GAL1-10 locus are controlled by separable, interdependent mechanisms. Mol. Biol. Cell *27*, 2980–2993.

Brickner, J. (2017). Genetic and epigenetic control of the spatial organization of the genome. Mol. Biol. Cell *28*, 364–369.

Brickner, J.H., and Fuller, R.S. (1997). SOI1 encodes a novel, conserved protein that promotes TGN-endosomal cycling of Kex2p and other membrane proteins by modulating the function of two TGN localization signals. J. Cell Biol. *139*, 23–36.

Brickner, J.H., and Walter, P. (2004). Gene recruitment of the activated INO1 locus to the nuclear membrane. PLoS Biol. *2*, e342.

Buchwalter, A.L., Liang, Y., and Hetzer, M.W. (2014). Nup50 is required for cell differentiation and exhibits transcription-dependent dynamics. Mol. Biol. Cell *25*, 2472–2484.

Burke, D., Dawson, D., and Stearns, T. (2000). Methods in Yeast Genetics (Cold Spring Harbor Press).

Cabal, G.G., Genovesio, A., Rodriguez-Navarro, S., Zimmer, C., Gadal, O., Lesne, A., Buc, H., Feuerbach-Fournier, F., Olivo-Marin, J.C., Hurt, E.C., et al. (2006). Saga interacting factors confine sub-diffusion of transcribed genes to the nuclear envelope. Nature *441*, 770–773.

Casolari, J.M., Brown, C.R., Drubin, D.A., Rando, O.J., and Silver, P.A. (2005). Developmentally induced changes in transcriptional program alter spatial organization across chromosomes. Genes Dev. *19*, 1188–1198.

Casolari, J.M., Brown, C.R., Komili, S., West, J., Hieronymus, H., and Silver, P.A. (2004). Genome-wide localization of the nuclear transport machinery couples transcriptional status and nuclear organization. Cell *117*, 427–439.

Chowdhary, S., Kainth, A.S., and Gross, D.S. (2017). Heat shock protein genes undergo dynamic alteration in their three-dimensional structure and genome organization in response to thermal stress. Mol. Cell. Biol. *37*.

Cremer, T., and Cremer, M. (2010). Chromosome territories. Cold Spring Harb. Perspect. Biol. *2*, a003889.

Dieppois, G., Iglesias, N., and Stutz, F. (2006). Cotranscriptional recruitment to the mRNA export receptor Mex67p contributes to nuclear pore anchoring of activated genes. Mol. Cell. Biol. *26*, 7858–7870.

Dilworth, D.J., Tackett, A.J., Rogers, R.S., Yi, E.C., Christmas, R.H., Smith, J.J., Siegel, A.F., Chait, B.T., Wozniak, R.W., and Aitchison, J.D. (2005). The mobile nucleoporin Nup2p and chromatin-bound Prp20p function in endogenous NPC-mediated transcriptional control. J. Cell Biol. *171*, 955–965.

Drysdale, C.M., Dueñas, E., Jackson, B.M., Reusser, U., Braus, G.H., and Hinnebusch, A.G. (1995). The transcriptional activator GCN4 contains multiple activation domains that are critically dependent on hydrophobic amino acids. Mol. Cell. Biol. *15*, 1220–1233.

Dultz, E., Tjong, H., Weider, E., Herzog, M., Young, B., Brune, C., Müllner, D., Loewen, C., Alber, F., and Weis, K. (2016). Global reorganization of budding yeast chromosome conformation in different physiological conditions. J. Cell Biol. *212*, 321–334.

D'Urso, A., Takahashi, Y.H., Xiong, B., Marone, J., Coukos, R., Randise-Hinchliff, C., Wang, J.P., Shilatifard, A., and Brickner, J.H. (2016). Set1/COMPASS and Mediator are repurposed to promote epigenetic transcriptional memory. Elife *5*.

Edelman, L.B., and Fraser, P. (2012). Transcription factories: genetic programming in three dimensions. Curr. Opin. Genet. Dev. *22*, 110–114.

Egecioglu, D., and Brickner, J.H. (2011). Gene positioning and expression. Curr. Opin. Cell Biol. *23*, 338–345.

Egecioglu, D.E., D'Urso, A., Brickner, D.G., Light, W.H., and Brickner, J.H. (2014). Approaches to studying subnuclear organization and gene-nuclear pore interactions. Methods Cell Biol. *122*, 463–485.

Eskiw, C.H., Cope, N.F., Clay, I., Schoenfelder, S., Nagano, T., and Fraser, P. (2010). Transcription factories and nuclear organization of the genome. Cold Spring Harb. Symp. Quant. Biol. *75*, 501–506.

Fraser, P., and Bickmore, W. (2007). Nuclear organization of the genome and the potential for gene regulation. Nature *447*, 413–417.

Green, E.M., Jiang, Y., Joyner, R., and Weis, K. (2012). A negative feedback loop at the nuclear periphery regulates GAL gene expression. Mol. Biol. Cell *23*, 1367–1375.

Haeusler, R.A., Pratt-Hyatt, M., Good, P.D., Gipson, T.A., and Engelke, D.R. (2008). Clustering of yeast tRNA genes is mediated by specific association of condensin with tRNA gene transcription complexes. Genes Dev. *22*, 2204–2214.

Harr, J.C., Luperchio, T.R., Wong, X., Cohen, E., Wheelan, S.J., and Reddy, K.L. (2015). Directed targeting of chromatin to the nuclear lamina is mediated by chromatin state and A-type lamins. J. Cell Biol. *208*, 33–52.

Haruki, H., Nishikawa, J., and Laemmli, U.K. (2008). The anchor-away technique: rapid, conditional establishment of yeast mutant phenotypes. Mol. Cell *31*, 925–932.

Hinnebusch, A.G. (1997). Translational regulation of yeast GCN4. J. Biol. Chem. *272*, 21661–21664.

Hinnebusch, A.G., and Fink, G.R. (1983). Positive regulation in the general amino acid control of Saccharomyces cerevisiae. Proc. Natl. Acad. Sci. USA *80*, 5374–5378.

Hope, I.A., Mahadevan, S., and Struhl, K. (1988). Structural and functional characterization of the short acidic transcriptional activation region of yeast GCN4 protein. Nature *333*, 635–640.

Hope, I.A., and Struhl, K. (1986). Functional dissection of a eukaryotic transcriptional activator protein, GCN4 of yeast. Cell *46*, 885–894.

Hu, Y., Plutz, M., and Belmont, A.S. (2010). Hsp70 gene association with nuclear speckles is Hsp70 promoter specific. J. Cell Biol. *191*, 711–719.

Huh, W.K., Falvo, J.V., Gerke, L.C., Carroll, A.S., Howson, R.W., Weissman, J.S., and O'Shea, E.K. (2003). Global analysis of protein localization in budding yeast. Nature *425*, 686–691.

Ibarra, A., and Hetzer, M.W. (2015). Nuclear pore proteins and the control of genome functions. Genes Dev. *29*, 337–349.

Ikegami, K., and Lieb, J.D. (2013). Integral nuclear pore proteins bind to Pol III-transcribed genes and are required for Pol III transcript processing in C. elegans. Mol. Cell *51*, 840–849.

Kalverda, B., and Fornerod, M. (2010). Characterization of genome-nucleoporin interactions in Drosophila links chromatin insulators to the nuclear pore complex. Cell Cycle *9*, 4812–4817.

Kalverda, B., Pickersgill, H., Shloma, V.V., and Fornerod, M. (2010). Nucleoporins directly stimulate expression of developmental and cell-cycle genes inside the nucleoplasm. Cell *140*, 360–371.

Kim, S., Liachko, I., Brickner, D.G., Cook, K., Noble, W.S., Brickner, J.H., Shendure, J., and Dunham, M.J. (2017). The dynamic three-dimensional organization of the diploid yeast genome. Elife *6*.

Liang, Y., Franks, T.M., Marchetto, M.C., Gage, F.H., and Hetzer, M.W. (2013). Dynamic association of NUP98 with the human genome. PLoS Genet. *9*, e1003308.

Light, W.H., Brickner, D.G., Brand, V.R., and Brickner, J.H. (2010). Interaction of a DNA zip code with the nuclear pore complex promotes H2A.Z incorporation and INO1 transcriptional memory. Mol. Cell *40*, 112–125.

Longtine, M.S., McKenzie, A., 3rd, Demarini, D.J., Shah, N.G., Wach, A., Brachat, A., Philippsen, P., and Pringle, J.R. (1998). Additional modules for versatile and economical PCR-based gene deletion and modification in Saccharomyces cerevisiae. Yeast *14*, 953–961.

Lucchini, G., Hinnebusch, A.G., Chen, C., and Fink, G.R. (1984). Positive regulatory interactions of the HIS4 gene of Saccharomyces cerevisiae. Mol. Cell. Biol. *4*, 1326–1333.

Luthra, R., Kerr, S.C., Harreman, M.T., Apponi, L.H., Fasken, M.B., Ramineni, S., Chaurasia, S., Valentini, S.R., and Corbett, A.H. (2007). Actively transcribed GAL genes can be physically linked to the nuclear pore by the SAGA chromatin modifying complex. J. Biol. Chem. *282*, 3042–3049.

Meinema, A.C., Laba, J.K., Hapsari, R.A., Otten, R., Mulder, F.A., Kralt, A., van den Bogaart, G., Lusk, C.P., Poolman, B., and Veenhoff, L.M. (2011). Long unfolded linkers facilitate membrane protein import through the nuclear pore complex. Science *333*, 90–93.

Mueller, P.P., Harashima, S., and Hinnebusch, A.G. (1987). A segment of GCN4 mRNA containing the upstream AUG codons confers translational control upon a heterologous yeast transcript. Proc. Natl. Acad. Sci. USA *84*, 2863–2867.

Noma, K., Cam, H.P., Maraia, R.J., and Grewal, S.I. (2006). A role for TFIIIC transcription factor complex in genome organization. Cell *125*, 859–872.

Parada, L.A., McQueen, P.G., and Misteli, T. (2004). Tissue-specific spatial organization of genomes. Genome Biol. *5*, R44.

Pascual-Garcia, P., Jeong, J., and Capelson, M. (2014). Nucleoporin Nup98 associates with Trx/MLL and NSL histone-modifying complexes and regulates Hox gene expression. Cell Rep. *9*, 433–442.

Raices, M., Bukata, L., Sakuma, S., Borlido, J., Hernandez, L.S., Hart, D.O., and D'Angelo, M.A. (2017). Nuclear pores regulate muscle development and maintenance by assembling a localized Mef2C complex. Dev. Cell *41*, 540–554.e7.

Randise-Hinchliff, C., and Brickner, J.H. (2016). Transcription factors dynamically control the spatial organization of the yeast genome. Nucleus *7*, 369–374.

Randise-Hinchliff, C., Coukos, R., Sood, V., Sumner, M.C., Zdraljevic, S., Meldi Sholl, L., Garvey Brickner, D., Ahmed, S., Watchmaker, L., and Brickner, J.H. (2016). Strategies to regulate transcription factor–mediated

gene positioning and interchromosomal clustering at the nuclear periphery. J. Cell Biol. *212*, 633–646.

Rawal, Y., Chereji, R.V., Valabhoju, V., Qiu, H., Ocampo, J., Clark, D.J., and Hinnebusch, A.G. (2018). Gcn4 binding in coding regions can activate internal and canonical 5′ promoters in yeast. Mol. Cell *70*, 297–311.e4.

Reja, R., Vinayachandran, V., Ghosh, S., and Pugh, B.F. (2015). Molecular mechanisms of ribosomal protein gene regulation. Genes Dev. *29*, 1942–1954.

Robinett, C.C., Straight, A., Li, G., Willhelm, C., Sudlow, G., Murray, A., and Belmont, A.S. (1996). In vivo localization of DNA sequences and visualization of large-scale chromatin organization using lac operator/repressor recognition. J. Cell Biol. *135*, 1685–1700.

Rudra, D., Zhao, Y., and Warner, J.R. (2005). Central role of Ifh1p-Fhl1p interaction in the synthesis of yeast ribosomal proteins. EMBO J. *24*, 533–542.

Sarma, N.J., Haley, T.M., Barbara, K.E., Buford, T.D., Willis, K.A., and Santangelo, G.M. (2007). Glucose-responsive regulators of gene expression in Saccharomyces cerevisiae function at the nuclear periphery via a reverse recruitment mechanism. Genetics *175*, 1127–1135.

Schmid, M., Arib, G., Laemmli, C., Nishikawa, J., Durussel, T., and Laemmli, U.K. (2006). Nup-PI: the nucleopore-promoter interaction of genes in yeast. Mol. Cell *21*, 379–391.

Schneider, M., Hellerschmied, D., Schubert, T., Amlacher, S., Vinayachandran, V., Reja, R., Pugh, B.F., Clausen, T., and Köhler, A. (2015). The nuclear pore-associated TREX-2 complex employs mediator to regulate gene expression. Cell *162*, 1016–1028.

Schoenfelder, S., Sexton, T., Chakalova, L., Cope, N.F., Horton, A., Andrews, S., Kurukuti, S., Mitchell, J.A., Umlauf, D., Dimitrova, D.S., et al. (2010). Preferential associations between co-regulated genes reveal a transcriptional interactome in erythroid cells. Nat. Genet. *42*, 53–61.

Sigler, P.B. (1988). Transcriptional activation. Acid blobs and negative noodles. Nature *333*, 210–212.

Sood, V., Cajigas, I., D'Urso, A., Light, W.H., and Brickner, J.H. (2017). Epigenetic transcriptional memory of GAL genes depends on growth in glucose and the Tup1 transcription factor in Saccharomyces cerevisiae. Genetics *206*, 1895–1907.

Spilianakis, C.G., Lalioti, M.D., Town, T., Lee, G.R., and Flavell, R.A. (2005). Interchromosomal associations between alternatively expressed loci. Nature *435*, 637–645.

Straight, A.F., Belmont, A.S., Robinett, C.C., and Murray, A.W. (1996). GFP tagging of budding yeast chromosomes reveals that protein-protein interactions can mediate sister chromatid cohesion. Curr. Biol. *6*, 1599–1608.

Taddei, A., Van Houwe, G., Hediger, F., Kalck, V., Cubizolles, F., Schober, H., and Gasser, S.M. (2006). Nuclear pore association confers optimal expression levels for an inducible yeast gene. Nature *441*, 774–778.

Takizawa, T., Meaburn, K.J., and Misteli, T. (2008). The meaning of gene positioning. Cell *135*, 9–13.

Van de Vosse, D.W., Wan, Y., Lapetina, D.L., Chen, W.M., Chiang, J.H., Aitchison, J.D., and Wozniak, R.W. (2013). A role for the nucleoporin Nup170p in chromatin structure and gene silencing. Cell *152*, 969–983.

van Steensel, B., and Belmont, A.S. (2017). Lamina-associated domains: links with chromosome architecture, heterochromatin, and gene repression. Cell *169*, 780–791.

Warfield, L., Tuttle, L.M., Pacheco, D., Klevit, R.E., and Hahn, S. (2014). A sequence-specific transcription activator motif and powerful synthetic variants that bind Mediator using a fuzzy protein interface. Proc. Natl. Acad. Sci. USA *111*, E3506–E3513.

Zullo, J.M., Demarco, I.A., Piqué-Regi, R., Gaffney, D.J., Epstein, C.B., Spooner, C.J., Luperchio, T.R., Bernstein, B.E., Pritchard, J.K., Reddy, K.L., et al. (2012). DNA sequence-dependent compartmentalization and silencing of chromatin at the nuclear lamina. Cell *149*, 1474–1487.

STAR★METHODS

KEY RESOURCES TABLE

REAGENT or RESOURCE	SOURCE	IDENTIFIER
Antibodies		
Anti GFP	Abcam	AB_2313768
Anti TAP	Life Technologies	AB_10709700
Anti LexA	Millipore Corporation	AB_310223
Dynabeads M-280 sheep anti-rabbit IgG	ThermoFisher	AB_2783009
Bacterial and Virus Strains		
DH5α		N/A
Chemicals, Peptides, and Recombinant Proteins		
All chemicals unless otherwise noted	Sigma-Aldrich	N/A
Yeast media components	Sunrise Science Products	N/A
Rapamycin	Millipore Corporation	553210
Hygromycin B	Gold Biotechnology	H-270-5-1
G418	Santa Cruz Biotechnology	Sc-29065A
UTP	Enzo life sciences	ENZ-42844
Restriction Enzymes	New England Biolabs	N/A
Critical Commercial Assays		
QuantSeq 3′ mRNA-Seq Library Prep Kit FWD	Illumina	N/A
Nick translation kit	Enzo life sciences	ENZ-42910
Pierce BCA Assay kit	Fisher scientific	PI23223
Deposited Data		
Details in Table S18	NCBI Accession ID PRJNA541268	N/A
Experimental Models: Organisms/Strains		
Saccharomyces cerevisiae	See Strain Tables S8–S16	N/A
Oligonucleotides		
See Oligo Table S17	Integrated DNA Technologies	N/A
Synthetic genes	Integrated DNA Technologies	N/A
Recombinant DNA		
Plasmids	Reference	
pAFS144	Straight et al., 1996	N/A
pFA6a-KanMX6	Longtine et al., 1998	N/A
p5LacI-GFP	Egecioglu et al., 2014	N/A
pER04	Egecioglu et al., 2014	N/A
pZipKan	Egecioglu et al., 2014	N/A
p6LacO128	Brickner and Walter, 2004	N/A
p6-LacO128-LexABS	Randise-Hinchliff et al., 2016	N/A
p6LacO128-HIS4	Randise-Hinchliff et al., 2016	N/A
pADH-LexA	Randise-Hinchliff et al., 2016	N/A
pRS305-PHO88-mCherry	D'Urso et al., 2016	N/A
pFA6a-FRB-GFP-His5MX	Haruki et al., 2008	N/A
pADH1-GCN4	this study	N/A
pGAL1-LexA	this study	N/A
p6LacO128-RPS0A	this study	N/A
p6LacO128-RPS1B	this study	N/A
p6LacO128-RPS6A	this study	N/A
p6LacO128-ALD3	this study	N/A

(*Continued on next page*)

Continued

REAGENT or RESOURCE	SOURCE	IDENTIFIER
p6LacO128-CTT1	this study	N/A
p6LacO128-GRE1	this study	N/A
p6LacO128-PDC1	this study	N/A
p6LacO128-PDC5	this study	N/A
p6LacO128-SSA2	this study	N/A
p6LacO128-SSA4	this study	N/A
p6LacO128-TMA10	this study	N/A
p6LacO128-UBI4	this study	N/A
p7-GFPrepI-LexADBD	this study	N/A
Software and Algorithms		
R studio	N/A	N/A
TrimmomaticSE	N/A	N/A
Tophat2	N/A	N/A
edgeR Bioconductor	N/A	N/A
LAS AF	N/A	N/A
Cufflinks	N/A	N/A
Cutadapt	N/A	N/A

CONTACT FOR REAGENT AND RESOURCE SHARING

Further information and requests for resources and reagents should be directed to and will be fulfilled by the Lead Contact, Jason Brickner (j-brickner@northwestern.edu).

EXPERIMENTAL MODEL AND SUBJECT DETAILS

Saccharomyces cerevisiae cultures were grown in YPD at 30°C unless otherwise noted. *E. coli* cultures were grown in LB+ Ampicilliin at 37°C.

METHOD DETAILS

Chemicals and Media and Growth Conditions

Unless specified, chemicals were from Sigma-Aldrich (St. Louis, MO), restriction and modifying enzymes were from New England Biolabs (Ipswich, MA), DNA oligonucleotides were from Integrated DNA Technologies (Skokie, IL), yeast media components were from Sunrise Science Products (San Diego, CA). Media were prepared as described (Burke et al., 2000). Unless indicated otherwise, yeast cultures were grown at 30°C in synthetic complete glucose (SDC) medium. For chromatin localization experiments, cells were grown at room temperature in YPD overnight and then shifted to SDC for $\geq$ 1h before imaging. Experiments with *HIS4* or *ILV2* were grown in SDC-His or SDC-Leu, respectively, to induce gene expression. Anchor Away experiments were cultured overnight in YPD or SDC then treated with 1μg/ml rapamycin for times indicated prior to confocal microscopy. Selection against *URA3-SUP4-o* was performed on SDC + 0.1% 5-fluoroorotate (FOA) plates (Randise-Hinchliff et al., 2016).

Yeast Strains, Plasmids and Molecular Biology

All yeast strains were derived from the W303 strains CRY1 (*MAT***a** *ade2-1 ura3-1 trp1-1 his3-11,15 leu2-3,112 can1-100*) or CRY2 (*MATα ade2-1 ura3-1 trp1-1 his3-11,15 leu2-3,112 can1-100*; Brickner and Fuller, 1997), BY4741 (*MAT***a** *his3Δ1 leu2Δ0 lys2Δ0 ura3Δ0*) or HHY168 (*MATα tor1-1 fpr1::NAT RPL13A-2×FKBP12::TRP1 ura3-1 trp1-1 his3-11,15 leu2-3,112 can1-100*) and are listed in Table S7 (strains used for the Heh2-mCherry screen), S8 (strains used for the Pho88-mCherry screen), S9, and S10 (no LexA BS strains), S11 and S12 (*nup2** mutant positives), S13 and S14 (*nup100** mutant positives) and S15 (other strains used in this study).

Plasmids pAFS144 (Straight et al., 1996), pFA6a-kanMX6 (Longtine et al., 1998), p5LacI-GFP, pER04, pZipKan (Egecioglu et al., 2014), p6LacO128 (Brickner and Walter, 2004), p6LacO128-LexABS, p6LacO128-HIS4, pADH-LexA (Randise-Hinchliff et al., 2016) pRS305-Pho88-mCherry (D'Urso et al., 2016) and pFA6a-FRB-GFP-His5MX (Haruki et al., 2008) have been previously described. New LacO array plasmids (p6LacO128-RPS0A, p6LacO128-RPS1B, p6LacO128-RPS6A, and p6LacO128-ILV2) were generated as described (Brickner et al., 2010): 1kb downstream of the genes was cloned into p6LacO128 using *Bam*HI and *Not*I restriction sites.

These plasmids were digested with enzymes with unique sites in the 1kb fragment to integrate. Plasmid pADH1-GCN4 was derived from pXRA2 (Addgene # 63144); an overhanging PCR fusing P_{ADH} with primers AAGCTTTAATAGGCGCATGCAACTTC and CTTGTCATCGTCGTCCTTGTAGTCCAT with the CDS and 410bp of 3' UTR of *GCN4* was inserted into pXRA2 as a *Hin*dIII-*Xho*I fragment. Wild type and mutant versions of the PD_{GCN4} were cloned as synthetic DNA oligonucleotides into plasmid pGAL1-LexA, which was derived from pRSII402 (Addgene # 35434). A gBLOCK (IDT) bearing the entire *GAL1-10* promoter and LexA DNA binding domain was inserted as a *Kpn*I-*Xba*I fragment. C-terminal LexA fusions were introduced as *Hin*dIII-*Xho*I fragments between the promoter and the LexA DBD. To integrate this plasmid at *ADE2*, the plasmid was linearized with *Stu*I.

To introduce the *pd* mutation at the endogenous *GCN4*, a PCR product with the mutation was transformed into a strain with *URA3-SUP4*-o inserted into *GCN4* (Randise-Hinchliff et al., 2016) and selected on 5-fluoroorotic acid. The mutation was confirmed by PCR on their genomic DNA and sequencing.

To generate transcription factor-LexA DBD fusion proteins in strains from the GFP collection (p7-GFPrepI-LexADBD) a gBLOCK (IDT) was cloned with 36bp of homology to the GFP tag upstream of the LexA DBD, followed by a 332bp 3'UTR from the *ACT1* gene, followed by the RPL13A promoter driving expression of the *KmR* gene, followed by 252bp 3'UTR from the *ADH1* gene (which is also downstream of the *His5+* marker in the GFP-tagged strain collection). This gBLOCK was amplified by PCR and transformed into 187 strains having DNA binding proteins tagged with GFP. Transformants were plated on YPD containing G418, screened for –His as well as imaged by confocal microscopy for the loss of the nuclear GFP signal. Proper fusion and expression of selected TF-LexA DBD proteins was confirmed by PCR and DNA sequencing as well as western blot against LexA DBD. The 187 *MAT***a** LexA DBD fusion protein strains were crossed against *MAT*α strains expressing LacI-GFP with the nuclear envelope and cortical ER labeled with mCherry and having either p6LacO128-LexABS or p6LacO128 integrated at *URA3*. Diploid strains were selected on SDC –Ade, -Ura plates.

CRISPR/ Cas-9 Mutagenesis

To mutagenize *NUP2* and *NUP100* in yeast diploid cells, guide RNA (gRNA) plasmids were generated by introducing duplexed oligonucleotides with homology to specific genomic loci near known PAM sequences with overhanging *Bpl*I sites into pBRA89 cut with *Bpl*I (Thermo Fisher Scientific, product number ER1311). Yeast strains were then co-transformed with gRNA plasmid and repair DNA for nup2* (5'-AATACAGAGAGAAACGTACGATTCTAACGAGTCTGACTGAAGGTTGCGTCATCTGCTGTGATGAATAGAA GAAAAATTGC) or nup100* (5'-TACTAACAATGTTTGGCAACAATAGACCAATGTTTTGAGGGAGCAACCTTTCCTTTCAACAATCG CAACAACCAAACTCTCTTTTTG) and plated on YPD + Hygromycin B. The nup2* introduces a stop codon and a 19bp deletion/ frameshift, truncating the protein after amino acid 21. The nup100* mutation introduces a stop codon and a 27bp deletion, truncating the protein after amino acid 9. Hygromycin-positive colonies were screened for the desired mutation either by yeast colony PCR or genomic preps followed by PCR with primers that could discern mutant from wildtype genotypes.

Confocal Microscopy

Cultures were grown as described, and 1μl was spotted onto a microscope slide and visualized on a Leica SP5 or SP8 as described in the Northwestern University Biological Imaging Facility (Egecioglu et al., 2014). Z-stacks of $\geq$ 5μm, comprising the whole yeast cell, were collected. For experiments in which we scored peripheral localization, 30–50 cells were scored per biological replicate and at least three biological replicates were scored for each strain or condition. Similarly, for experiments in which we measured the distance between two loci, we only analyzed cells with 1) two visible dots and 2) in which both dots were in the same Z-slice. Cells were excluded if they had abnormal nuclear morphology or more than two dots. Distances between two loci were measured using LAS AF software.

Anchor Away

Anchor Away experiments were performed as described in D'Urso et al. (2016). Cells cultured overnight in YPD or SDC then treated with 1μg/ml rapamycin for times indicated prior to confocal microscopy.

Chromatin Immunoprecipitation (ChIP)

ChIP experiments were performed as described (Egecioglu et al., 2014) with the following modifications. Strains expressing fragments of *GCN4* fused to LexA DBD under the control of the *GAL1-10* promotor were grown overnight in YPD, then diluted to 0.2 OD_{600} and switched to YPG for 3 hrs to induce protein expression. Cells were fixed for 20 min with 1% formaldehyde. Protein was immunoprecipitated using 5 μL of Pan-Rabbit IgG magnetic beads and 3 μL of anti-LexA antibody, and rotated for overnight at 4°C. Recovery was quantified relative to input by real-time quantitative PCR with primers used to amplify the LexA BS and the *PRM1* CDS.

RT-qPCR and RNAseq

Wild type, *gcn4-pd* mutant and *gcn4Δ* strains were grown overnight at 30°C in SDC. The culture was diluted to $OD_{600} \sim$ 0.3-0.4 and shifted either to SDC as a control or SDC-His to induce *HIS4* gene expression for 1.5h. Approximately 5 x 10^7 cells were harvested, RNA was extracted, treated with DNAase and reverse transcribed and quantified by quantitative PCR as described (Brickner et al., 2007).

RNAseq samples (2-3 replicates of each condition and strain) were prepared using QuantSeq 3' mRNA-Seq Library Prep Kit FWD for Illumina (Lexogen, NH) following the manufacturer's instructions. Sequencing was performed with an Illumina Hiseq (Illumina, San Diego, CA) at the Northwestern University NUSeq core facility. Approximately 120 Mb of 50 bp single-end reads were generated for each condition. The first 8-bp were cropped from the raw reads using TrimmomaticSE and the adapter sequences were trimmed by Cutadapt. The trimmed reads were mapped to the *S. cerevisiae* genome (SacCer3) using Tophat2 and only uniquely aligned reads were retained. FPKM (fragments per kilobase of exon model per million reads mapped) of the annotated genes was calculated by Cufflinks. Differential expression analysis was performed using the exact test of the edgeR Bioconductor package. Genes that gave no detectable reads were removed from further analysis.

DNA FISH

CRY1 was grown overnight to mid-log phase (OD 0.5) and fixed in 5% formaldehyde for 2 h. Cells were treated with lyticase, permeablized and adhered to poly-lysine treated slides as described in Brickner et al. (2007). Cells were allowed to settle on the slide for 15 min before incubation with prehybridization buffer at 37°C for 1 h. Ten x 500bp probes covering the *RPS0A* locus were synthesized using a nick translation kit and red580 UTP (Enzo, ENZ-42844). Probes were concentrated, pooled and denatured according to manufacturer's instructions. Samples were incubated with probe overnight at 37°C, washed several times with a dilution series of 2XSSC buffer. Nuclei were stained with DAPI for 5 min at room temperature and washed several times. Mounting media and a cover slip was applied before samples were imaged on a confocal microscope. Peripheral localization of the *RPS0A* locus was assessed in 50 cells.

QUANTIFICATION AND STATISTICAL ANALYSIS

All statistical analysis was performed using R version 3.5.2. In Figure 1, Student's t-test was used to compare with WT (Figures 1A–1C and 1G), with 0 min time point (Figures 1E and 1F) or to the *PRM1* control (D). In Figure 2, Student's t-test to compare to the LexA strain (Figures 2A and 2G), to the WT strain (Figures 2B, 2H, and 2I), to the *PRM1* control (Figure 2E); L. Fold induction of Gcn4 target genes, with mean and standard deviation, compared with Student's t-test. In Figure 3B, we compared ± LexA BS (WT) or to WT (*nup2* & *nup100*) using Student's t-test Figure S3B modeled the bimodal distribution from the tethering screen, the distribution was iteratively analyzed using the *mixtools* package, starting with estimated means of 32% and 55%, lambda of 0.5 and scalar (sigsrd) = 25. The final fit required 12 iterations (Heh2 screen) or 29 iterations (Poh88 screen). For Figure 4A TF targets from YeastMine were compared with nuclear pore binding sites from published datasets (Casolari et al., 2004, 2005; Van de Vosse et al., 2013). Predicted and observed overlap was compared using the Fisher Exact test. The distributions of P-values among positives and negatives was also compared with a Student's t-test. In Figures 4D and 4E, Student's t test was used to compare uninducing and inducing conditions. Figure 5 and B the percent localization of each gene was compared to that of *URA3* (A) or to the 0-minute time point (B) with t-test. In Figures 5C and 5D the P-values are from Fisher test (bar graphs) or Kolmogorov-Smirnov test (violin plots).

For the simulation of positions generated for Figure S1A, 10,000 positions were generated within a 2μm x 2μm cube and then filtered for those contained within a 2μm diameter sphere (n = 5200). The slice (right) represents the subset of these 5200 positions that are within 0.2μm of the equator of the sphere. To generate a simulation of distances between these positions, 1000 positions were randomly selected to be the first position and 1000 positions were randomly selected to be the second position and the 3D distance between them was calculated.

DATA AND SOFTWARE AVAILABILITY

All R scripts used for data analysis are available as Markdowns upon request. RNAseq data were deposited into the NCBI Short Reads Database (https://www.ncbi.nlm.nih.gov/sra), accession # PRJNA541268 and BioSample IDs are detailed in Table S18.